Viscous potential flow analysis of capillary instability with heat and mass transfer

2008 J. Phys. A: Math. Theor. 41 335205

(http://iopscience.iop.org/1751-8121/41/33/335205)

IOP PUBLISHING JOURNAL OF PHYSICS A: MATHEMATICAL AND THEORETICAL

J. Phys. A: Math. Theor. **41** (2008) 335205 (11pp) doi:10.1088/1751-8113/41/33/335205

Viscous potential flow analysis of capillary instability with heat and mass transfer

H J Kim[1], S J Kwon[1], Juan C Padrino[2] and Toshio Funada[3]

[1] Department of Aerospace Engineering, KAIST, 373-1 Guseong-dong, Yuseong-gu, Daejeon, 305-701, Korea
[2] Department of Aerospace Engineering and Mechanics, University of Minnesota, Minneapolis, MN 55455, USA
[3] Department of Digital Engineering, Numazu College of Technology, Ooka 3600, Numazu, Shizuoka 410-8501, Japan

E-mail: elquin.hjk@gmail.com

Received 11 April 2008, in final form 10 June 2008
Published 15 July 2008
Online at stacks.iop.org/JPhysA/41/335205

Abstract

We carry out the linear viscous-irrotational analysis of capillary instability with heat transfer and phase change. We consider the cylindrical interface shared by two viscous incompressible fluids enclosed by two concentric cylinders. In viscous potential flow, viscosity enters the model through the balance of normal stresses at the interface. We write the dispersion relation from the stability analysis for axisymmetric disturbances in terms of a set of dimensionless numbers that arise in this phase change problem. For the film boiling condition, plots depicting the effect of some of these parameters on the maximum growth rate for unstable perturbations and critical wavenumber for marginal stability are presented and interpreted. Viscous effects of a purely irrotational motion in the presence of heat and mass transfer can stabilize an otherwise unstable gas–liquid interface.

PACS numbers: 47.20.Ma, 47.20.Gv, 47.55.N–

1. Introduction

The problem of Rayleigh–Taylor and Kelvin–Helmholtz instability with heat and mass transfer across the liquid–vapor interface was formulated for potential flow of an inviscid fluid by Hsieh [1, 2]. He modeled 'small' perturbations of a plane interface between two fluids bounded by two parallel plates. Hsieh [2] found that when the vapor layer is hotter than the liquid layer, the presence of heat and mass transfer mitigates, but does not suppress the growth of unstable perturbations; however, the classical stability criterion remains unaltered. Regarding Kelvin–Helmholtz instability, the classical stability criterion is modified when heat and mass transfer are included in the analysis, although the heat flux does not appear in the relation.

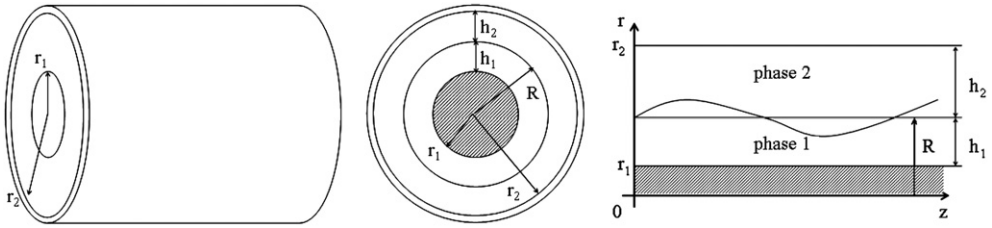

Figure 1. Schematic of stability analysis.

Nayak and Chakraborty [3] studied the Kelvin–Helmholtz stability of the cylindrical interface between the liquid and vapor phases with heat and mass transfer. Lee [4, 5] studied Rayleigh and Kelvin–Helmholtz instabilities in phase change problems with mass transfer for the fluid motion in a cylindrical pipe flow and in a channel, respectively. In both cases, Lee found that the nonlinear stability criterion is strongly sensitive to the amount of heat transfer, contrary to the linear results by Hsieh [2]. Moreover, Lee's results show that in the nonlinear case the region of stability is bounded above and below, unlike the linear case, which depicts a single neutral curve. All these investigations assumed that the flow is irrotational and the fluid inviscid (inviscid potential flow (IPF)).

Recently, Asthana and Agrawal [6] carried out the potential flow analysis of the Kelvin–Helmholtz instability with heat and mass transfer for two viscous fluids confined between two parallel planes. They presented a stability criterion given by a critical relative velocity. They also found that heat and mass transfer has a stabilizing effect when the lower fluid is highly viscous, whereas it has a destabilizing effect when the lower fluid has a low viscosity. Their work is an extension to include heat and mass transfer phenomena of the study of Kelvin–Helmholtz instability of two viscous fluids by Funada and Joseph [7].

In this paper, we investigate the capillary instability problem of a vapor–liquid system in an annular configuration with heat and mass transfer using viscous potential flow (VPF) for axisymmetric disturbances. We follow Hsieh's [2] analysis, assume irrotational motion but, unlike Hsieh, we do not set the fluid viscosity to zero. Therefore, the viscous part of the normal stress enters the analysis; however, the non-slip condition at the boundary is not enforced for irrotational flow. As in Hsieh [2], we assume that the phase change is induced by an interfacial condition for energy transfer which balances the latent heat against conductive heat transfer (see (9)), thereby neglecting convection. An antecedent of this work is the study by Funada and Joseph [8], who carried out the viscous potential flow analysis of capillary instability of a cylindrical core of fluid surrounded by another fluid with no heat and mass transfer. They found the condition, in terms of a dimensionless number based on the relevant parameters of the system, for which the growth rate from viscous potential flow closely approaches the solution of the linearized Navier–Stokes equations. Their results show that viscous potential flow is a better approximation of the exact solution than the inviscid model. This motivates the assumption of viscous irrotational motion to carry out the present stability analysis involving phase change and heat transfer. A comprehensive discussion of the theory of viscous potential flow, with numerous examples, can be found in the recent book by Joseph, Funada and Wang [9].

2. Problem formulation

We consider two fluids separated by a cylindrical interface in an annular configuration as in figure 1. Both phases 1 and 2 are considered incompressible and irrotational. In the equilibrium

state, the inner fluid region $r_1 < r < R$ has thickness h_1, density ρ_1 and viscosity μ_1 and the outer fluid region $R < r < r_2$ has thickness h_2, density ρ_2 and viscosity μ_2. The boundary surfaces at $r = r_1$ and $r = r_2$ are considered to be rigid. The temperatures at $r = r_1, r = R$ and $r = r_2$ are T_1, T_0 and T_2, respectively. In the basic state, thermodynamics equilibrium is assumed and the interface temperature T_0 is set equal to the saturation temperature.

Small axisymmetric disturbances are superimposed to the basic state of rest. In the disturbed state, the interface is thus given by

$$F(r, z, t) = r - R - \eta(z, t) = 0, \tag{1}$$

where η is the perturbation in the radius of the interface from its equilibrium value. The velocity is expressed as the gradient of a potential and the potential functions satisfy Laplace's equation as a consequence of the incompressibility constraint. That is,

$$\nabla^2 \phi_i = 0 \qquad (i = 1, 2). \tag{2}$$

These potentials are periodic in z.

We assume that phase-change takes place locally in such a way that the net phase-change rate at the interface is equal to zero. The interfacial condition, which expresses the conservation of mass across the interface, is given by

$$\left[\!\left[\rho_i \left(\frac{\partial F}{\partial t} + \nabla \phi_i \cdot \nabla F \right) \right]\!\right] = 0, \tag{3}$$

where $[\![x]\!] = x_{R^+} - x_{R^-}$ represents the difference in a quantity as we cross the interface. Then, by use of (1), (3) becomes

$$\left[\!\left[\rho_i \left(\frac{\partial \phi_i}{\partial r} - \frac{\partial \eta}{\partial t} - \frac{\partial \eta}{\partial z} \frac{\partial \phi_i}{\partial z} \right) \right]\!\right] = 0 \qquad \text{at} \quad r = R + \eta. \tag{4}$$

With mass transfer across the interface, the normal stress balance becomes, at $r = R + \eta$,

$$\begin{aligned} \rho_1 (\nabla \phi_1 \cdot \nabla F) \left(\frac{\partial F}{\partial t} + \nabla \phi_1 \cdot \nabla F \right) &= \rho_2 (\nabla \phi_2 \cdot \nabla F) \left(\frac{\partial F}{\partial t} + \nabla \phi_2 \cdot \nabla F \right) \\ &+ (p_2 - p_1 - 2\mu_2 \boldsymbol{n} \cdot \nabla \otimes \nabla \phi_2 \cdot \boldsymbol{n} + 2\mu_1 \boldsymbol{n} \cdot \nabla \otimes \nabla \phi_1 \cdot \boldsymbol{n} + \sigma \nabla \cdot \boldsymbol{n}) |\nabla F|^2, \end{aligned} \tag{5}$$

where p is the pressure, σ is the surface tension coefficient and $\boldsymbol{n}$ is the normal vector at the interface, respectively. Surface tension has been assumed to be a constant, neglecting its dependence upon temperature, and thereby ignoring any Marangoni effect.

The pressure in (5) may be obtained from Bernoulli's equation. When this is done, (5) becomes, at $r = R + \eta$,

$$\begin{aligned} \left[\!\left[\rho_i \left\{ \frac{\partial \phi_i}{\partial t} + \frac{1}{2} \left(\frac{\partial \phi_i}{\partial r} \right)^2 + \frac{1}{2} \left(\frac{\partial \phi_i}{\partial z} \right)^2 - \left[1 + \left(\frac{\partial \eta}{\partial z} \right)^2 \right]^{-1} \left(\frac{\partial \phi_i}{\partial r} - \frac{\partial \eta}{\partial z} \frac{\partial \phi_i}{\partial z} \right) \right.\right.\right. \\ \left.\left.\left. \times \left(\frac{\partial \phi_i}{\partial r} - \frac{\partial \eta}{\partial t} - \frac{\partial \eta}{\partial z} \frac{\partial \phi_i}{\partial z} \right) \right\} + 2\mu_i \left[\frac{\partial^2 \phi_i}{\partial r^2} - 2 \frac{\partial \eta}{\partial z} \frac{\partial^2 \phi_i}{\partial r \partial z} + \frac{\partial^2 \phi_i}{\partial z^2} \left(\frac{\partial \eta}{\partial z} \right)^2 \right] \right]\!\right] \\ = \sigma \nabla \cdot \boldsymbol{n}, \end{aligned} \tag{6}$$

using (1). At the wall the normal velocity vanishes, hence,

$$\frac{\partial \phi_1}{\partial r} = 0 \qquad \text{at} \quad r = r_1, \tag{7}$$

$$\frac{\partial \phi_2}{\partial r} = 0 \qquad \text{at} \quad r = r_2. \tag{8}$$

The perturbed heat flux at the interface $r = R + \eta(z, t)$ induces phase change. The interfacial condition for this energy transfer proposed by Hsieh [2] is expressed as

$$L\rho_1 \left(\frac{\partial F}{\partial t} + \nabla\phi_1 \cdot \nabla F \right) = S(\eta) \qquad \text{at} \quad r = R + \eta, \tag{9}$$

where L is the latent heat released from the fluid when is transformed from phase 1 to phase 2 and $S(\eta)$ denotes the net heat flux from the interface. Hsieh [2] indicates that:

> 'The expression $S(\eta)$ essentially represents the net heat flux from the interface when such a phase transformation is taking place. In general, the heat fluxes have to be determined from equations governing the heat transfer in the fluids, thus completely coupling the dynamics and the thermal exchanges in the entire flow region. In this simplified version, ... S is simply a function of η, and moreover, S is to be determined from the heat exchange relations in the equilibrium state.'

In the equilibrium state, the heat fluxes in the positive r-direction in the fluid phases 1 and 2 are expressed as $-K_1(T_1 - T_0)/R\ln(r_1/R)$ and $-K_2(T_0 - T_2)/R\ln(R/r_2)$, respectively where K_1 and K_2 are the heat conductivities of the two fluids. After Hsieh [2], Nayak and Chakraborty [3] wrote this expression for the cylindrical geometry,

$$S(\eta) = \frac{K_2(T_0 - T_2)}{(R + \eta)[\ln r_2 - \ln(R + \eta)]} - \frac{K_1(T_1 - T_0)}{(R + \eta)[\ln(R + \eta) - \ln r_1]}, \tag{10}$$

and expand it in a Taylor series about $r = R$ as

$$S(\eta) = S(0) + \eta S'(0) + \tfrac{1}{2}\eta^2 S''(0) + \cdots. \tag{11}$$

Then, we take $S(0) = 0$, so that

$$G = \frac{K_2(T_0 - T_2)}{R\ln(r_2/R)} = \frac{K_1(T_1 - T_0)}{R\ln(R/r_1)} = \frac{(T_1 - T_2)/R}{\ln(R/r_1)/K_1 + \ln(r_2/R)/K_2} \tag{12}$$

indicating that in the equilibrium state the heat fluxes are equal across the vapor–liquid interface. Although the problem has been defined in a somewhat general framework, one can picture the situation of a boiling liquid layer in contact with one of the boundary surfaces and its vapor, considered incompressible, in contact with the other surface. Then, one may apply the model detailed here to the vapor–liquid interface.

3. Solution of the linearized problem

Linearization of the relations (4), (6) and (9) yields

$$\left[\!\left[\rho_i \left(\frac{\partial\phi_i}{\partial r} - \frac{\partial\eta}{\partial t} \right) \right]\!\right] = 0, \tag{13}$$

$$\left[\!\left[\rho_i \frac{\partial\phi_i}{\partial t} + 2\mu_i \frac{\partial^2\phi_i}{\partial r^2} \right]\!\right] = -\sigma \left(\frac{\partial^2\eta}{\partial z^2} + \frac{\eta}{R^2} \right), \tag{14}$$

$$\rho_1 \left(\frac{\partial\phi_1}{\partial r} - \frac{\partial\eta}{\partial t} \right) = \alpha\eta, \tag{15}$$

at $r = R$, where (10)–(12) have been used to obtain (15) and

$$\alpha = \frac{G}{LR} \frac{\ln(r_2/r_1)}{\ln(R/r_1)\ln(r_2/R)}. \tag{16}$$

Additionally, Hsieh [2] notes that the '... vapor phase is usually hotter than the liquid phase; therefore α is always positive'.

From Laplace's equation (2), in cylindrical coordinates, we can write for the harmonic potential $\phi_i(r, z)$, $(i = 1, 2)$,

$$\nabla^2\phi_i = \frac{\partial^2\phi_i}{\partial r^2} + \frac{1}{r}\frac{\partial\phi_i}{\partial r} + \frac{\partial^2\phi_i}{\partial z^2} = 0, \tag{17}$$

with boundary conditions (7) at the wall.

We use standard normal mode decomposition to find solutions of the above set of governing equations. Let

$$\eta = C\exp(\mathrm{i}kz - \mathrm{i}\omega t) + \text{c.c.} = CE + \text{c.c.}, \tag{18}$$

where C is constant, $E \equiv \exp(\mathrm{i}kz - \mathrm{i}\omega t)$, i is the imaginary unit, k is the real wavenumber, $\omega = \omega_R + \mathrm{i}\omega_I$ is the complex frequency and c.c. represents the complex conjugate of the previous term. Hence, solutions for the velocity potential have the form

$$\begin{aligned}\phi_1 &= \frac{1}{k}\left(\frac{\alpha}{\rho_1} - \mathrm{i}\omega\right)A_0(k, r)CE + \text{c.c.},\\ \phi_2 &= \frac{1}{k}\left(\frac{\alpha}{\rho_2} - \mathrm{i}\omega\right)B_0(k, r)CE + \text{c.c.},\end{aligned} \tag{19}$$

where

$$\begin{aligned}A_0(k, r) &= \frac{I_0(kr)K_1(kr_1) + I_1(kr_1)K_0(kr)}{I_1(kR)K_1(kr_1) - I_1(kr_1)K_1(kR)},\\ B_0(k, r) &= \frac{I_0(kr)K_1(kr_2) + I_1(kr_2)K_0(kr)}{I_1(kR)K_1(kr_2) - I_1(kr_2)K_1(kR)},\end{aligned}$$

and I_n, K_n are modified Bessel functions of the first and second kind. In writing (19), constraints (13) and (14) have been satisfied.

4. Dispersion relation

4.1. Dimensional form

Substituting (18) and (19) into (14), we find

$$D(\omega, k) = a_0\omega^2 + \mathrm{i}a_1\omega + a_2 = 0, \tag{20}$$

where

$$\begin{aligned}a_0 &= \rho_1 A_0(k, R) - \rho_2 B_0(k, R),\\ a_1 &= \alpha[A_0(k, R) - B_0(k, R)] + 2k^2[\mu_1 A_t(k, R) - \mu_2 B_t(k, R)],\\ a_2 &= -\sigma k\left(k^2 - \frac{1}{R^2}\right) - 2\alpha k^2\left[\frac{\mu_1}{\rho_1}A_t(k, R) - \frac{\mu_2}{\rho_2}B_t(k, R)\right],\\ A_t(k, R) &= A_0(k, R) - \frac{1}{kR},\\ B_t(k, R) &= B_0(k, R) - \frac{1}{kR}.\end{aligned}$$

For $\omega = \omega_R + \mathrm{i}\omega_I$, the quadratic equation (20) is separated into the real and imaginary parts. After eliminating ω_R, we obtain the following expression for the growth rate ω_I:

$$a_0\omega_I^2 + a_1\omega_I - a_2 = 0. \tag{21}$$

Neutral curves, $\omega_I(k) = 0$, are generated by the condition $a_2 = 0$, which implies

$$\sigma\left(k_c^2 - \frac{1}{R^2}\right) + 2\alpha k_c\left[\frac{\mu_1}{\rho_1}A_t(k_c, R) - \frac{\mu_2}{\rho_2}B_t(k_c, R)\right] = 0, \tag{22}$$

where k_c denotes the critical wavenumber. Expression (22) reveals that the effects of heat and mass transfer carried by α enters into the definition of the neutral curve if the viscous effects of the irrotational motion are considered in the analysis. For inviscid potential flow (see also Lee [4]), the critical wavenumber $k_c = 1/R$ is independent of α. For zero heat flux ($\alpha = 0$), both VPF and IPF predicts the same k_c.

4.2. Dimensionless form

To write the dispersion relation in dimensionless form we introduce the following dimensionless groups:

$$\hat{r} = r/H, \qquad \hat{z} = z/H, \qquad \hat{\eta} = \eta/H,$$
$$\hat{t} = t/\tau, \qquad \hat{\omega} = \omega\tau, \qquad \hat{k} = kH,$$
$$\varphi = \frac{h_1}{H}, \qquad \hat{R} = \hat{r}_1 + \varphi,$$

where the length scale H and the time scale τ are defined as

$$H = h_1 + h_2 = r_2 - r_1,$$
$$\tau = \sqrt{\frac{\rho_2 H^3}{\sigma}},$$

and φ denotes the dimensionless vapor thickness. Furthermore,

$$\ell = \frac{\rho_1}{\rho_2}, \qquad m = \frac{\mu_1}{\mu_2},$$
$$\kappa = \frac{\nu_1}{\nu_2} = \frac{m}{\ell} \qquad \text{with} \quad \nu_1 = \frac{\mu_1}{\rho_1}, \quad \nu_2 = \frac{\mu_2}{\rho_2},$$

and

$$Oh = \frac{\sqrt{\rho_2\sigma H}}{\mu_2}, \qquad \hat{\alpha} = \frac{\alpha}{\rho_2/\tau},$$

where Oh is the Ohnesorge number and $\hat{\alpha}$ denotes the heat-transfer capillary group. Note that surface tension, which is essential in the description of the phenomena, is contained in these two-dimensionless groups.

Eliminating the '^' on the dimensionless variables for brevity, (20) may be written in dimensionless form as

$$D(\omega, k) = a_0\omega^2 + \mathrm{i}a_1\omega + a_2 = 0, \tag{23}$$

where

$$a_0 = \ell A_0(k, R) - B_0(k, R),$$
$$a_1 = \alpha[A_0(k, R) - B_0(k, R)] + \frac{2}{Oh}k^2[mA_t(k, R) - B_t(k, R)],$$
$$a_2 = -k\left(k^2 - \frac{1}{R^2}\right) - \frac{2\alpha}{Oh}k^2\left[\frac{m}{\ell}A_t(k, R) - B_t(k, R)\right].$$

From (22), the expression for the neutral curve becomes

$$\left(k_c^2 - \frac{1}{R^2}\right) + \Lambda k_c[\kappa A_t(k_c, R) - B_t(k_c, R)] = 0, \tag{24}$$

with an alternative heat-transfer capillary dimensionless group

$$\Lambda = \frac{2\alpha}{Oh}, \tag{25}$$

which is introduced for convenience.

From (24), we can define $f(k)$ for fixed R as

$$f(k) \equiv \left(k^2 - \frac{1}{R^2}\right) + \Lambda k[\kappa A_t(k, R) - B_t(k, R)]. \tag{26}$$

From (26), if we let the third term $\Lambda k[\kappa A_t(k, R) - B_t(k, R)]$ as $g(k)$, then $g(k) = g(-k)$. Then we can say that $f(k) = f(-k)$, $f(0)$ is a minimum and $f(k)$ is concave. Thus $f(0) < 0$ is a necessary condition for which k_c ($k_c > 0$) exists. When a real $k_c > 0$ cannot be obtained, the fluid configuration is stable.

For $k \sim 0$, the asymptotic form of $f(k)$ is

$$(k^2R^2 - 1) + \Lambda R^2 \left[\kappa\left(\frac{2R}{R^2 - r_1^2} - \frac{1}{R}\right) + \frac{2R}{r_2^2 - R^2} + \frac{1}{R}\right] = 0. \tag{27}$$

Then, there is no critical wavenumber $k_c > 0$ under the following condition for which $f(0) > 0$:

$$\Lambda R^2 \left[\kappa\left(\frac{2R}{R^2 - r_1^2} - \frac{1}{R}\right) + \left(\frac{2R}{r_2^2 - R^2} + \frac{1}{R}\right)\right] > 1 \tag{28}$$

or

$$\Lambda R \left[\kappa\left(\frac{R^2 + r_1^2}{R^2 - r_1^2}\right) + \frac{R^2 + r_2^2}{r_2^2 - R^2}\right] > 1. \tag{29}$$

5. Computation and discussion of results—viscous stabilization of water–steam systems

In this section, we carry out computations using the expressions presented in the previous sections for a film boiling condition. We take water and steam as working fluids. Referring to figure 1, the steam and water are identified with phase 1 and phase 2, respectively, such that $T_1 > T_0 > T_2$. In film boiling, the water–steam interface is in saturation condition and the temperature T_0 is set equal to the saturation temperature. The properties of both phases are determined for this condition. The diameter of the inner and outer cylinder is 1 mm and 2 mm, respectively. By knowing the vapor thickness and two temperatures of the triad (T_0, T_1, T_2), the heat flux and the unknown temperature can be predicted from the conduction model (12).

The results from the stability analysis of capillary instability with heat and mass transfer are presented in table 1 for comparing the maximum growth rate ω_{Im}, related wavenumber k_m and critical wavenumber k_c as a function of the heat-transfer capillary number α (dimensionless) for IPF and VPF. The difference between the α scales is due to the change of dimensionless vapor thickness φ, from 0.01 to 0.1. This table confirms that the maximum growth rate for IPF and VPF decreases as α increases, with ω_{Im} from VPF decreasing more fast. Also, VPF renders lower values of ω_{Im} than IPF for the same α. By comparing results for $\varphi = 0.01$ and $\varphi = 0.1$, we note that discrepancies between IPF and VPF substantially diminish as the vapor fraction increases. In this table, the last lines of results for $\varphi = 0.01$ and $\varphi = 0.1$ show the critical α for which $k_c = 0$ according to VPF, corresponding to a stable interface. Note that the threshold α for the thicker vapor thickness $\varphi = 0.1$ is larger than the critical α associated with the smaller $\varphi = 0.01$.

Table 1. Maximum growth rate parameters and critical wavenumber as a function of the heat-transfer-capillary number α and dimensionless vapor thickness φ according to (23) for the water–steam system ($\ell = 0.0015$, $m = 0.0604$ and $Oh = 1012$ obtained for $T_0 = 400$ K).

$\varphi = 0.01$						
	IPF			VPF		
α	ω_{Im}	k_m	k_c	ω_{Im}	k_m	k_c
0.0000	0.4891	0.6672	0.9804	0.4855	0.6646	0.9804
0.0153	0.1375	0.6910	0.9804	0.1060	0.6448	0.9150
0.0305	0.0730	0.6924	0.9804	0.0406	0.5964	0.8446
0.0458	0.0493	0.6928	0.9804	0.0186	0.5424	0.7676
0.0610	0.0371	0.6928	0.9804	0.0087	0.4820	0.6820
0.0763	0.0298	0.6930	0.9804	0.0038	0.4128	0.5840
0.0916	0.0248	0.6930	0.9804	0.0000	0.0002	0.0002
0.1206	0.0189	0.6930	0.9804	0.0000	0.0000	0.0000
$\varphi = 0.10$						
	IPF			VPF		
α	ω_{Im}	k_m	k_c	ω_{Im}	k_m	k_c
0.0000	0.3661	0.5732	0.8334	0.3652	0.5724	0.8334
0.0010	0.3600	0.5736	0.8334	0.3588	0.5726	0.8330
0.0019	0.3540	0.5742	0.8334	0.3524	0.5728	0.8326
0.0029	0.3482	0.5746	0.8334	0.3462	0.5730	0.8320
0.0039	0.3424	0.5750	0.8334	0.3401	0.5732	0.8316
0.0048	0.3367	0.5754	0.8334	0.3340	0.5734	0.8312
0.0058	0.3312	0.5758	0.8334	0.3281	0.5734	0.8306
0.0068	0.3257	0.5762	0.8334	0.3223	0.5736	0.8302
12.143	0.0009	0.5878	0.8334	0.0000	0.0000	0.0000

Graphs of the critical wavenumber k_c versus the kinematic viscosity ratio κ are presented for various Λ values and $\varphi = 0.01$ in figure 2 related to (24). Here, the Müller method is used to find k_c in (24). We observe that for every Λ there exists a critical κ for which all waves are stable. This critical value decreases as the heat-transfer capillary number Λ increases. For an unstable system ($k_c > 0$), increasing κ for fixed Λ decreases the size of the interval of wavenumbers for unstable waves. k_c from VPF is bounded above by the inviscid result for all Λ.

Figure 3(*a*) shows the critical wavenumber k_c as a function of the dimensionless vapor thickness φ and heat-transfer capillary number Λ from (24) for $\kappa = 41.3218$ (water–steam at $T_0 = 400$ K). This shows that increasing Λ for fixed φ reduces the interval of unstable waves, which can be completely suppressed. By contrast, the graphs for the lower nonzero Λ ($= 0.1 \times 10^{-4}$ and 1.0×10^{-4}) reach the inviscid result for $\varphi > 0.2$, nearly. This result follows the tendency shown in table 1 for $\varphi = 0.1$. Figure 3(*b*) shows graphs of k_c versus φ for two values of Λ and κ. Note that while keeping Λ constant, increasing κ reduces k_c for fixed φ; hence, longer stable waves are predicted by the model. Through these results, the vapor thickness arises k_c increases when Λ increases for fixed κ and when κ decreases for fixed Λ. From the definition of Λ((25)), it is directly proportional to the heat flux and inversely proportional to surface tension. Therefore, when surface tension increases, the wavenumber interval for unstable waves becomes wider as Λ decreases for fixed κ (see figure 2).

Our results thus show that linear analysis of capillary instability with heat and mass transfer predicts a region of stability unbounded above ($k_c \leqslant k < \infty$) for viscous and inviscid

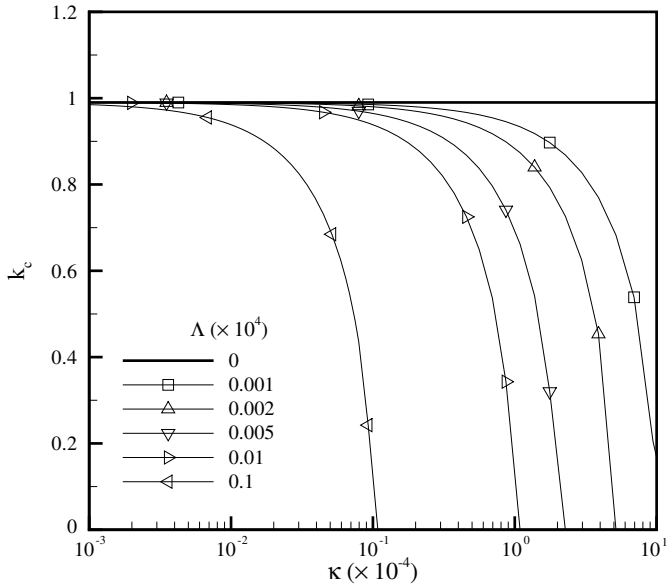

Figure 2. Critical wavenumber k_c versus kinematic viscosity ratio κ for a series of heat-transfer-capillary group Λ values and dimensionless vapor thickness $\varphi = 0.01$ according to (24). For every Λ, there is a critical κ above which all waves are stable.

potential flow, so that short waves are stable. In contrast, as shown by Lee [4], nonlinear inviscid analysis surprisingly predicts a region of stability with upper and lower bounds, thereby leading to both long and short unstable waves. Nevertheless, Lee's nonlinear analysis predicts that the width of the band of stability decreases by increasing the vapor thickness, and becomes wider by increasing the heat flux, trends that are similar to ours (see table 1).

In the frame of Hsieh's purely heat-conduction model, the effect of heat and mass transfer is explained in terms of local evaporation and condensation at the interface. At a perturbed interface, crests are warmer because they are closer to the hotter boundary on the vapor side, thus local evaporation occurs, whereas troughs are cooler and thus condensation takes place. A comprehensive discussion of phase-change effects in interfacial stability is presented by Ozen and Narayanan [10], who considered not only heat conduction but also convection. However, their system consisted of a liquid underlying its vapor between two parallel plates, where the plate in the liquid side is hotter. In this setup, the evaporation–condensation phenomena promote instability, which is mitigated by surface tension for short waves, in opposition to the physics described above for the system investigated in the present work.

A final remark on the assumption of irrotational motion is due. This approximation implies that the flow field does not satisfy the non-slip condition at the bounding surfaces and, consequently, the boundary layers at these locations are ignored. Similarly, vorticity layers on both sides of the interface are also disregarded and continuity of tangential velocity and stress at this position is not enforced. In making this assumption, we are encouraged by the results obtained by Funada and Joseph [8]. Using viscous potential flow as an approximation of the linearized Navier–Stokes analysis of capillary instability of a fluid cylinder in another fluid with no heat and mass transfer, they carried computations with more than a dozen of fluid pairs and concluded that VPF approximates the exact solution for gas–liquid or liquid–liquid flows when a dimensionless surface tension Oh^2 is greater than $O(10)$, where Oh is determined

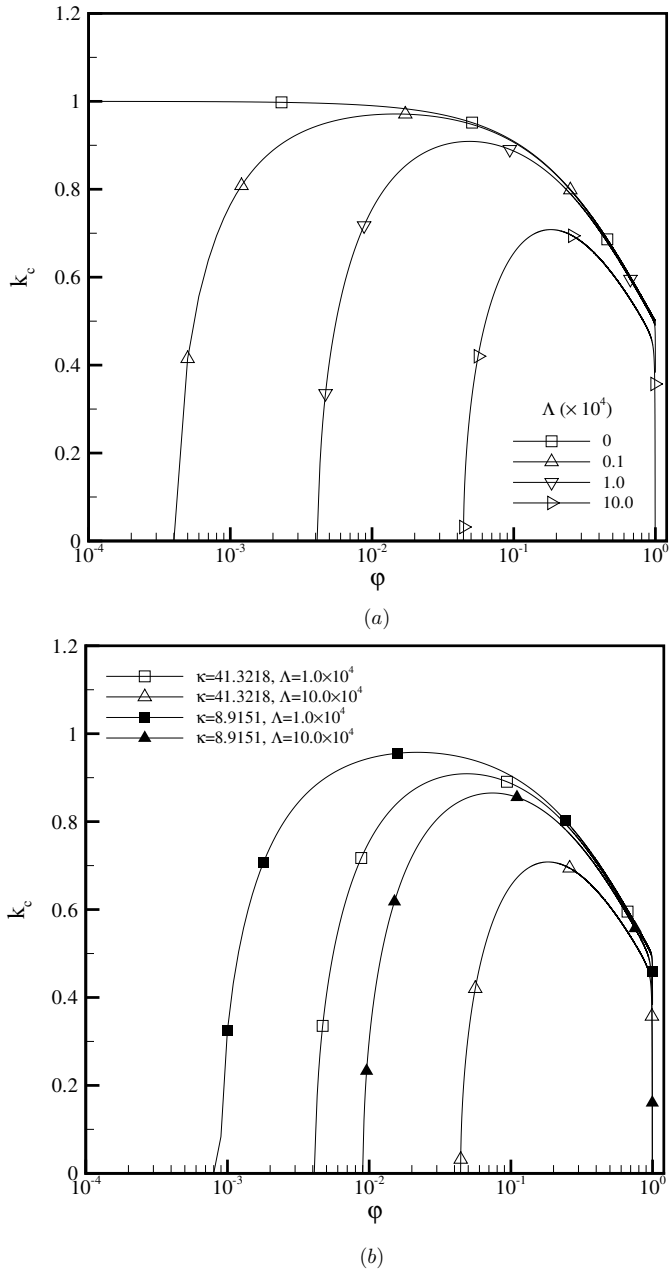

Figure 3. Critical wavenumber k_c versus dimensionless vapor thickness φ for different values of the heat-transfer-capillary number Λ according to (24) for the water–steam system: (*a*) for $\kappa = 41.3218$, $\ell = 0.0015$ and $Oh = 1012$ obtained for $T_0 = 400$ K; (*b*) comparison with graphs for $\kappa = 8.9151$, $\ell = 0.0159$ and $Oh = 1378$ obtained for $T_0 = 500$ K. The effects of heat and viscosity become outstanding for low vapor thickness.

with the properties of the most viscous fluid; otherwise, potential flow is off the mark and internal vorticity generation significantly affects the dynamics of the interface. In the frame

of the problem discussed here, boundary-layer flow impacts the interface stability through the diffusion of momentum and the transport of heat by convection in either side of the interface.

6. Conclusion

In this paper, we studied the capillary instability to linear perturbations of the cylindrical interface of two incompressible fluids confined in a concentric annulus with heat and mass transfer using viscous potential flow. Heat transfer is modeled exclusively as a conduction process. We obtained the dispersion relation describing the stability of the system in terms of various dimensionless numbers, namely density and viscosity ratios, dimensionless inner radius and phase fraction, the Ohnesorge number and a phase change parameter depending upon the geometry, the temperature difference, and fluid properties including latent heat. We applied the model to the film-boiling condition in which the liquid is in contact with the cooler outer boundary and its own vapor is in contact with the warmer inner boundary. Our main result is that, for the irrotational motion of two viscous fluids, heat and mass transfer phenomena can completely stabilize the interface against capillary effects. This conclusion cannot be achieved for inviscid fluids. Moreover, we found that the viscous effects of the irrotational motion interacting with heat and mass transfer reduce the maximum growth rate and increase the length of the wave with the maximum growth rate, in comparison with the inviscid case. As the vapor thickness increases, the difference between inviscid and viscous potential flow becomes less conspicuous.

Acknowledgments

H Kim wishes to thank Daniel D Joseph for his engaging discussions of matter related to this research. This work was supported by the Korea Science and Engineering Foundation (KOSEF) through the National Research Laboratory Program funded by the Ministry of Science and Technology (no R0A_2007_000_20065_0).

References

[1] Hsieh D Y 1972 Effects of heat and mass transfer on Rayleigh–Taylor instability *Trans. ASME, J. Basic, Eng.* **94D** 156
[2] Hsieh D Y 1978 Interfacial stability with mass and heat transfer *Phys. Fluids* **21** 745
[3] Nayak A R and Chakraborty B B 1984 Kelvin–Helmholtz stability with mass and heat transfer *Phys. Fluids* **27** 1937
[4] Lee D S 2003 Nonlinear Rayleigh instability of cylindrical flow with mass and heat transfer *J. Phys. A : Math. Gen.* **36** 573
[5] Lee D S 2005 Nonlinear Kelvin–Helmholtz instability of fluid layers with mass and heat transfer *J. Phys. A: Math. Gen.* **38** 2803
[6] Asthana R and Agrawal G S 2007 Viscous potential flow analysis of Kelvin–Helmholtz instability with mass transfer and vaporization *Phys. A : Stat. Mech. Appl.* **382** 389
[7] Funada T and Joseph D D 2001 Viscous potential flow analysis of Kelvin–Helmholtz instability in a channel *J. Fluid Mech.* **445** 263
[8] Funada T and Joseph D D 2002 Viscous potential flow analysis of capillary instability *Int. J. Multiph. Flow* **28** 1459
[9] Joseph D D, Funada T and Wang J 2007 *Potential Flows of Viscous and Viscoelastic Fluids* (Cambridge: Cambridge University Press)
[10] Ozen O and Narayanan R 2004 The physics of evaporative and convective instabilities in bilayer systems: linear theory *Phys. Fluids* **16** 4644
[11] Ozen O and Narayanan R 2004 The physics of evaporative instabilities in bilayer systems: weak non-linear theory *Phys. Fluids* **16** 4653